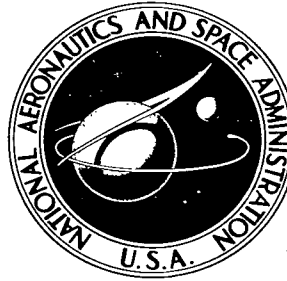


NASA TECHNICAL NOTE



NASA TN D-4278

C.1

LOAN COPY
GFWL W.
KIRK



NASA TN D-4278

LARGE-SCALE WIND-TUNNEL INVESTIGATION OF A MODEL WITH AN EXTERNAL JET-AUGMENTED FLAP

by Jerry V. Kirk, David H. Hickey, and Kiyoshi Aoyagi

Ames Research Center

Moffett Field, Calif.





LARGE-SCALE WIND-TUNNEL INVESTIGATION OF A MODEL WITH
AN EXTERNAL JET-AUGMENTED FLAP

By Jerry V. Kirk, David H. Hickey,
and Kiyoshi Aoyagi

Ames Research Center
Moffett Field, Calif.

NATIONAL AERONAUTICS AND SPACE ADMINISTRATION

For sale by the Clearinghouse for Federal Scientific and Technical Information
Springfield, Virginia 22151 - CFSTI price \$3.00

LARGE-SCALE WIND-TUNNEL INVESTIGATION OF A MODEL WITH AN EXTERNAL JET-AUGMENTED FLAP

By Jerry V. Kirk, David H. Hickey,
and Kiyoshi Aoyagi

Ames Research Center

SUMMARY

An investigation has been conducted in the Ames 40- by 80-Foot Wind Tunnel of a large-scale model powered by turbojet engines. The wing had 38.5° sweep of the leading edge, an aspect ratio of 5.38, a taper ratio of 0.23, and a dihedral of 3° . The wing airfoil section was an NACA 65-412. The trailing-edge flaps extended from 8 to 63 percent semispan. A small auxiliary flap spanned the main flap. The exhaust from the engines was directed against the flaps to augment lift.

Longitudinal aerodynamic characteristics for various combinations of main and auxiliary flap deflections are shown for thrust coefficients from 0 to approximately 1.4. Limited longitudinal and lateral-directional characteristics are shown for a simulated engine-out condition. Results also demonstrate the feasibility of using the small auxiliary flap as a means for providing direct-lift flight-path control.

INTRODUCTION

Various means have been proposed and studied for increasing the low-speed take-off and landing performance of high-speed jet aircraft. References 1 through 3 reported the use of an externally blown jet-augmented flap with the exhaust from propulsion engines directed against trailing-edge flaps to augment lift. Renewed interest in this method of increasing lift coefficient as a means for controlling flight path during steep landing approaches led to the present investigation.

A model with two turbojet engines exhausting against the wing trailing-edge flaps was employed in the investigation. During most of the tests, a small auxiliary flap was attached to the main flap. Conventional tail pipes were used on the jet engines, and the thrust axis was parallel to the wing chord plane. A paddle type exhaust deflector directed the exhaust to the slot between the wing and main flap. Longitudinal aerodynamic characteristics were determined for flap deflections of 10° , 20° , 40° , and 60° . At each main flap deflection with the exception of 60° , auxiliary-flap deflections from 20° to 40° were examined. Limited longitudinal and lateral-directional data are shown for simulated engine-out characteristics. The results were analyzed to ascertain the effect of using the auxiliary flap for directly controlling flight path.

NOTATION

A	wing aspect ratio, $\frac{b^2}{S}$
b	wing span, ft
c	wing chord parallel to plane of symmetry
\bar{c}	mean aerodynamic chord
C_l	rolling-moment coefficient, $\frac{l}{qSb}$
C_L	lift coefficient, $\frac{L}{qS}$
C_D	drag coefficient, $\frac{D}{qS}$
C_m	pitching-moment coefficient, $\frac{M}{qS\bar{c}}$
C_n	yawing-moment coefficient, $\frac{N}{qSb}$
C_y	side-force coefficient, $\frac{Y}{qS}$
D	drag, lb, total net force
F_g	gross thrust, lb
$\frac{F_g}{qS}$	thrust coefficient
$\frac{F_g}{W}$	thrust/gross weight ratio, $\frac{F_g/qS}{C_L}$
l	rolling moment, ft-lb
L	total lift on model, lb
M	pitching moment, ft-lb
N	yawing moment, ft-lb
q	free-stream dynamic pressure, lb/sq ft
R	Reynolds number

S	wing area, sq ft
V	free-stream air velocity, knots
W	gross weight, lb
Y	side force, lb
α	angle of attack of the wing-chord plane, deg
δ_D	jet exhaust deflector angle measured relative to the thrust axis, deg
δ_f	flap deflection measured in a streamwise direction relative to the wing-chord plane
δ_s	slat deflection measured relative to the wing-chord plane, deg
ρ	density, lb-sec ² /ft ⁴
η	fraction of wing semispan measured perpendicular to plane of symmetry
γ	flight-path angle, deg

Subscripts

aux	auxiliary flap
s	stall
u	uncorrected

MODEL

The model mounted for the tests on the normal strut system in the Ames 40- by 80-Foot Wind Tunnel is shown in figure 1. Sketches of the model showing pertinent details are presented in figure 2.

Fuselage

The fuselage was circular in cross section, the largest section being 4 feet in diameter.

Tail

The vertical tail had an NACA 0009 airfoil section. The horizontal tail, which had an NACA 64-009 airfoil section, was positioned near the top of the vertical tail and was set at zero incidence for the entire investigation.

Wing

The low mounted wing had a basic NACA 65-412 airfoil section with a trailing-edge-chord extension between stations $\eta = 0.109$ and $\eta = 0.366$ (ordinates shown on fig. 2(b)). The wing had a leading-edge sweep of 38.5° , aspect ratio of 5.38, taper ratio of 0.23, and 3° dihedral.

Engines

Two YJ85-5 turbojet engines were mounted in nacelles beneath the wing with the centerline of the thrust axis oriented parallel to the wing-chord plane; they were located laterally 5.2 feet from the fuselage centerline.

High-Lift Devices

Trailing-edge flaps extended from 8 to 63 percent of the wing semispan. The flaps were split at 37-percent semispan because of the change in wing trailing-edge sweep. The flap chord was 14 percent of the wing chord at the inboard station ($\eta = 0.08$) and 22 percent of the wing chord at wing station $\eta = 0.37$. A constant 22-percent chord was maintained from this juncture to the outboard tip of the flap at wing station $\eta = 0.63$. For a major portion of the test program a small auxiliary flap was attached to the main flap. The auxiliary flap chord was 33 percent of the main flap and spanned the entire main flap. Main-flap deflection was measured in a streamwise direction relative to the wing-chord plane. Auxiliary flap deflection was measured relative to the main-flap chord plane (fig. 2(c)).

Leading-edge slats extended the full span of the wing except the area enclosed by the engine nacelles. The slat chord was 15 percent of the wing chord. Deflections of 15° and 20° relative to the wing-chord plane with a 1.5-percent wing-chord gap were examined.

Jet-Exhaust Deflector

A paddle jet exhaust deflector was hinged aft of the engines on centerline to direct the exhaust into the flap slot.

TESTING PROCEDURE

Longitudinal force and moment data were obtained for angles of attack from -4° to $+32^\circ$ in the 40- by 80-foot wind tunnel. Limited lateral-directional results were obtained for the same range when differential thrust was applied to examine engine-out characteristics.

Model variables were flap deflection, leading-edge slat deflection, and differential engine thrust.

Thrust coefficient will be used as the independent parameter in the presentation of results. Free-stream dynamic pressure and engine thrust were varied to obtain thrust coefficients from 0 to approximately 1.4. Nominal values of dynamic pressure (q) for the various thrust coefficients examined were:

$\frac{F_g}{qS}$	q
0.25	32
.50	23
.70	16
1.0	11.2
1.35	8.5

Engine gross thrust measurements used in the computation of thrust coefficient were obtained from static calibrations of the engines using total pressure probes in the tailpipe. Thrust coefficient was held essentially constant as angle of attack was varied. Data were obtained for a range of thrust coefficients for each model configuration examined. Reynolds number varied from 4.3 to 8.2 million.

CORRECTIONS

All force and moment data were corrected for the effects of the wind-tunnel walls in the following manner:

$$\alpha = \alpha_u + 0.5234 C_{L_u}$$

$$C_D = C_{D_u} + 0.0091 C_{L_u}^2$$

$$C_m = C_{m_u} + 0.0150 C_{L_u}$$

The entire program was conducted without a fairing on the tail strut. Appropriate tare corrections have been applied to drag and pitching moment to account for this influence.

RESULTS

Table I is an index to the figures. Results with power off and the flaps up (auxiliary flap removed) are shown in figure 3 for both the leading-edge slats on and off. The variations in longitudinal characteristics for various main flap deflections with the auxiliary flap deflected 20° , 30° , or 40° are shown in figures 4 through 13. Results obtained with the flap deflected 60° and the auxiliary flap removed are shown in figure 14.

The effects on longitudinal characteristics of producing differential thrust to simulate engine-out characteristics are shown in figure 15 for two flap deflections and two thrust coefficients. The variations in lateral-directional characteristics for the engine-out conditions are shown in figure 16 for the same conditions presented in figure 15. Comparisons are made by showing symmetrical and asymmetrical thrust conditions near the same thrust coefficient. The simulation of one engine out for a four engine aircraft was accomplished by setting engine thrust and wind-tunnel speed for a nominal thrust coefficient of 1 and then reducing thrust on one engine to approximately half the value of the opposite engine. For a two engine aircraft the simulation was accomplished in a similar manner, but the thrust on one engine was reduced to that produced by windmill rpm.

DISCUSSION

In previous examinations of external jet flaps it was found necessary to direct the high-energy exhaust gases to the flap leading edge by such methods as tilting the engine thrust axis (ref. 1) or placing a deflector beneath the jet exhaust (ref. 2). Static results for the model of this investigation showed that a deflector of some sort was also needed to direct the engine-exhaust gas to the flap. A paddle type deflector was placed at the nozzle exit centerline and the best deflection angle was found to be 20° .

For all results shown, lift increased with increasing thrust coefficient. Engine operation and flap deflection did not significantly affect static margin or shift the pitching-moment curve below wing stall.

For descent with high thrust coefficients, large flap deflections are required. Results shown in figure 13 are for a flap deflection of 40° with the auxiliary flap deflected 40° . At a thrust coefficient of 1.36, a maximum lift coefficient of 4.3 was obtained with a corresponding drag coefficient of 0.95 at an angle of attack of 25° . These data correspond to a maximum descent angle of approximately 13° . At 0° angle of attack, a comparison of the data obtained at thrust coefficients of 0 and 1.36 shows that the incremental lift coefficient due to blowing is 1.8. If deflected thrust were used, the equivalent ΔC_L would be 1.36. Therefore 75 percent of the measured lift increment of 1.8 could be provided by the direct thrust of the deflected jet. With the flaps deflected $40^\circ/40^\circ$ ($\delta_f = 40^\circ$, $\delta_{f_{aux}} = 40^\circ$) the static turning angle of the jet stream was approximately 34° . Jet reaction (thrust coefficient $\times \sin 34^\circ$) divided by the measured lift increment of 1.8 shows that the flap actually converted approximately 43 percent of the jet reaction to lift so that the circulation and jet-lift components are nearly equal. The pitching-moment coefficient for the untrimmed maximum lift coefficient of 4.3 is -1.3. The corresponding trimmed value of maximum lift is 3.8 which represents a lift loss of about 11 percent due to trim requirements.

The feasibility of direct flight-path control by means of a small fast-acting auxiliary flap was reported in reference 4 and is shown in figure 17. Flight-path angle, in both climbing and descending flight, is presented as a function of flight speed for an assumed wing loading of 70 pounds per square


foot and a constant thrust/weight ratio of 0.4. The flight speed is based on a 20-percent speed margin above the trimmed stall speeds. The solid lines on figure 17 are obtained directly from experimental results with the main flap deflections of 10° , 20° , and 40° ; the dashed line of 30° was obtained by interpolation. Auxiliary flap deflection (from 20° to 40°) is the primary variable along any one line on figure 17. Changes in angle of attack for the flap deflections shown are small. Angle of attack varied from 7° to 11° for a flap deflection change from $40^\circ/40^\circ$ to $10^\circ/20^\circ$. Figure 17 shows that auxiliary flap deflection changes of 20° changed flight path about 4° . Flight path changes of 6° or more appear to be attainable by increasing the deflection range of the auxiliary from 0° to 50° . For a main flap deflection of 30° , at a constant flight speed and constant thrust, direct flight-path control from about a 4° descent angle to a 2° climb angle appears feasible.

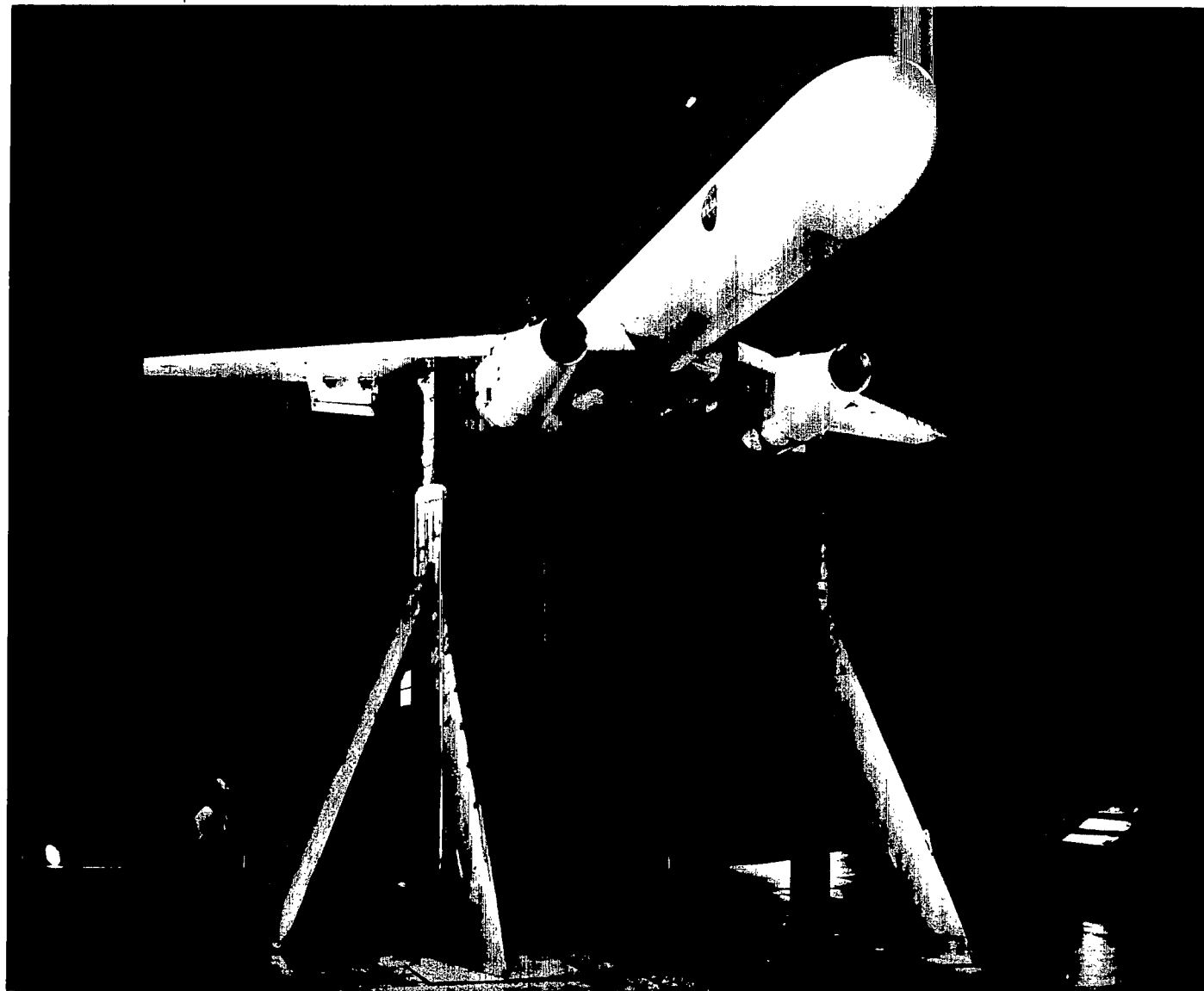
Ames Research Center
National Aeronautics and Space Administration
Moffett Field, Calif., 94035, Sept. 29, 1967
721-01-00-14-00-21

REFERENCES

1. Fink, Marvin P.: Aerodynamic Characteristics, Temperature, and Noise Measurements of a Large-Scale External-Flow Jet-Augmented-Flap Model With Turbojet Engines Operating. NASA TN D-943, 1961.
2. Campbell, John P.; and Johnson, Joseph L., Jr.: Wind-Tunnel Investigation of an External-Flow Jet-Augmented Slotted Flap Suitable for Application to Airplanes With Pod-Mounted Jet Engines. NACA TN 3898, 1956.
3. Johnson, Joseph L., Jr.: Wind-Tunnel Investigation of the Static Longitudinal Stability and Trim Characteristics of a Sweptback-Wing Jet-Transport Model Equipped With an External-Flow Jet-Augmented Flap. NACA TN 4177, 1958.
4. Deckert, Wallace H.; Koenig, David G.; and Weiberg, James A.: A Summary of Recent Large-Scale Research on High-Lift Devices. NASA SP-116, 1966, pp. 63-79.

TABLE I.- LIST OF FIGURES

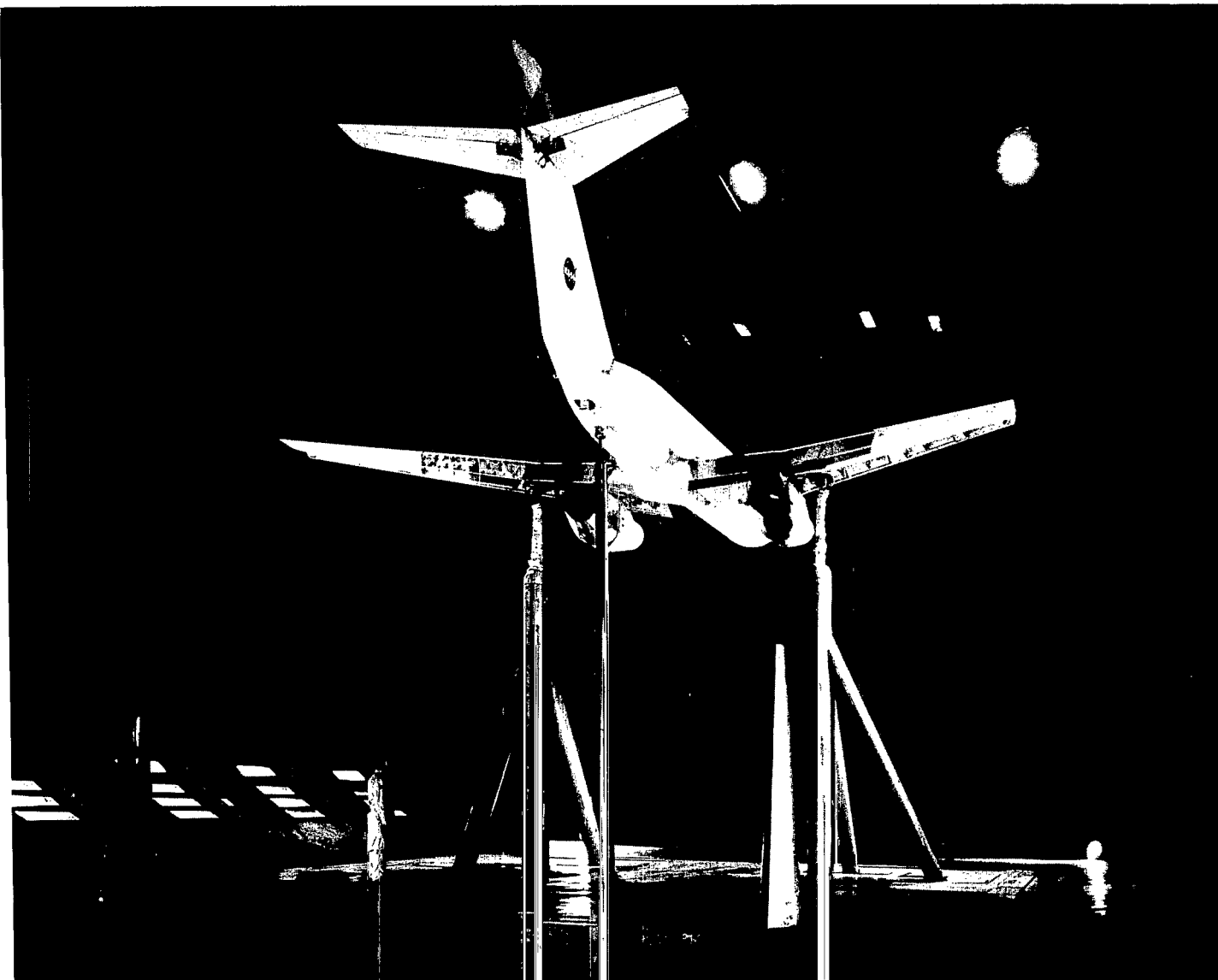
Figure	δ_f , deg	$\delta_{f_{aux}}$, deg	δ_D , deg	δ_s , deg	Remarks
3	0	Off	20	20 inboard 15 outboard and off	Power off
4	10	20	20	20	Power on 
5	10	30	20	20	
6	10	40	20	20	
7	20	20	20	20	
8	20	30	20	20	
9	20	40	20	20	
10	40	20	20	20	
11	40	30	20	20	
12	40	40	20	20	
13	40	40	20	20 inboard 15 outboard	
14	60	Off	20	20 inboard 15 outboard	
One engine-out simulation, longitudinal characteristics					
15(a)	10,40	30	20	20	Four engine aircraft
15(b)	40	30	20	20	Two engine aircraft
One engine-out simulation, lateral-directional characteristics					
16(a)	10	30	20	20	Four engine aircraft
16(b)	40	30	20	20	Four engine aircraft
16(c)	40	30	20	20	Two engine aircraft



(a) Three-quarter front view.

A-34818

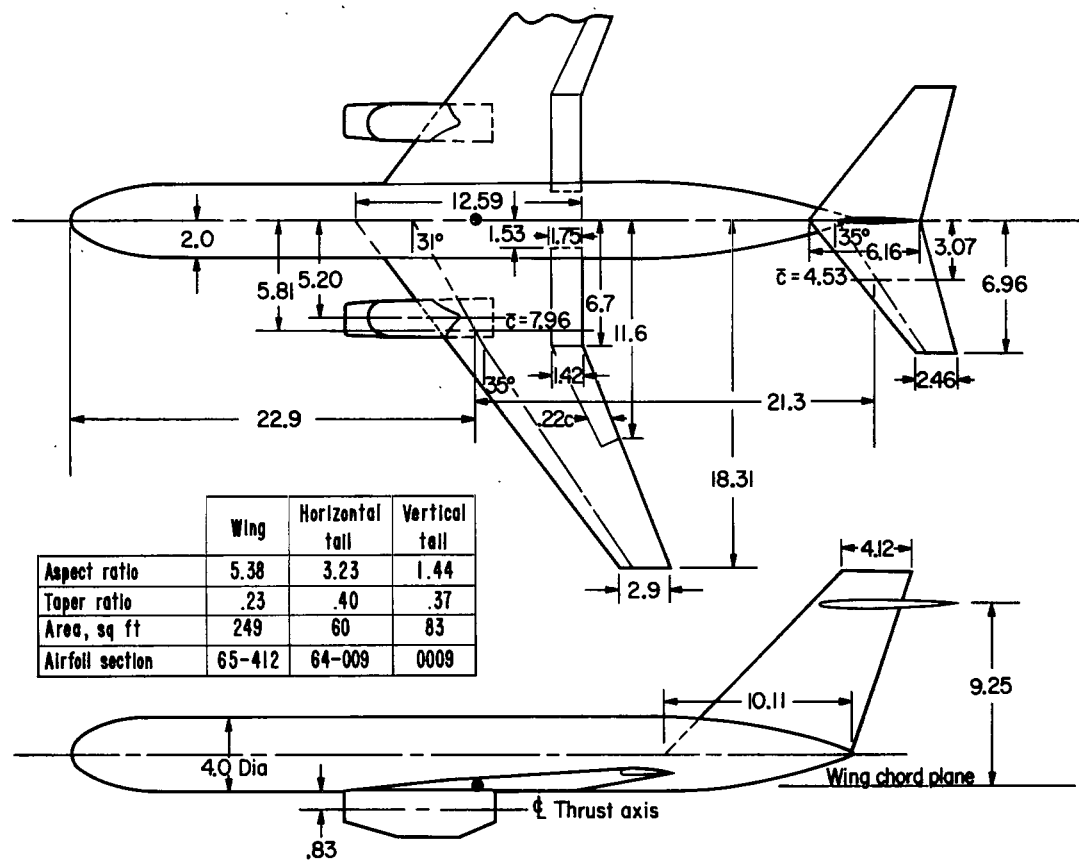
6 Figure 1.- Photographs of the model mounted in the test section of the Ames 40- by 80-Foot Wind Tunnel.



(b) Three-quarter rear view.

A-34819

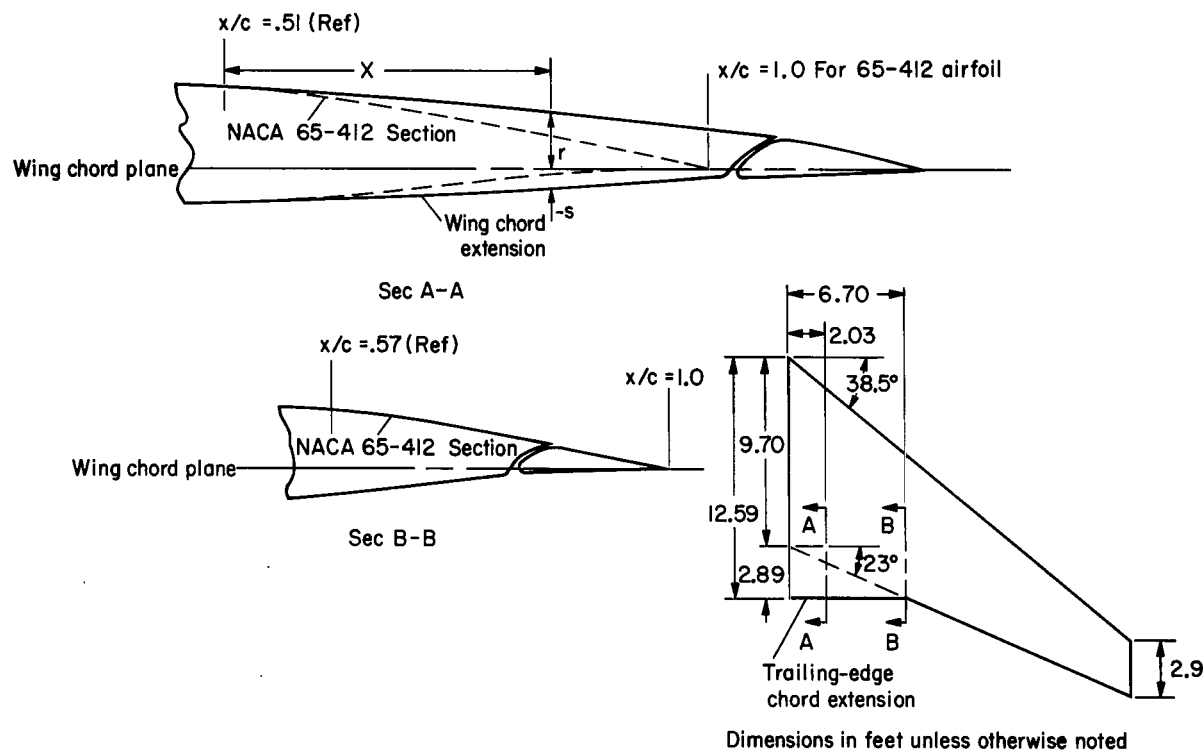
Figure 1.- Concluded.



Dimensions in feet unless otherwise noted

(a) Model geometry.

Figure 2.- Geometric details of the jet augmented flap model.



Sec A-A

Chord extension		
x, in.	r, in.	s, in.
0	8.50	-3.80
5.45	8.15	-3.53
17.45	7.30	-2.95
28.45	6.40	-2.32
41.45	5.52	-1.75
53.45	4.40	-1.06
55.20	4.21	0
56.45	4.05	1.55
57.45	3.90	2.35
58.95	3.70	3.10

Flap		
x, in.	r, in.	s, in.
55.45	-.43	-.43
56.15	1.03	-.93
57.45	2.23	-.76
58.45	3.14	—
60.65	3.30	—
62.24	3.12	-.29
66.95	2.09	.10
71.75	1.05	.28
76.60	0	0

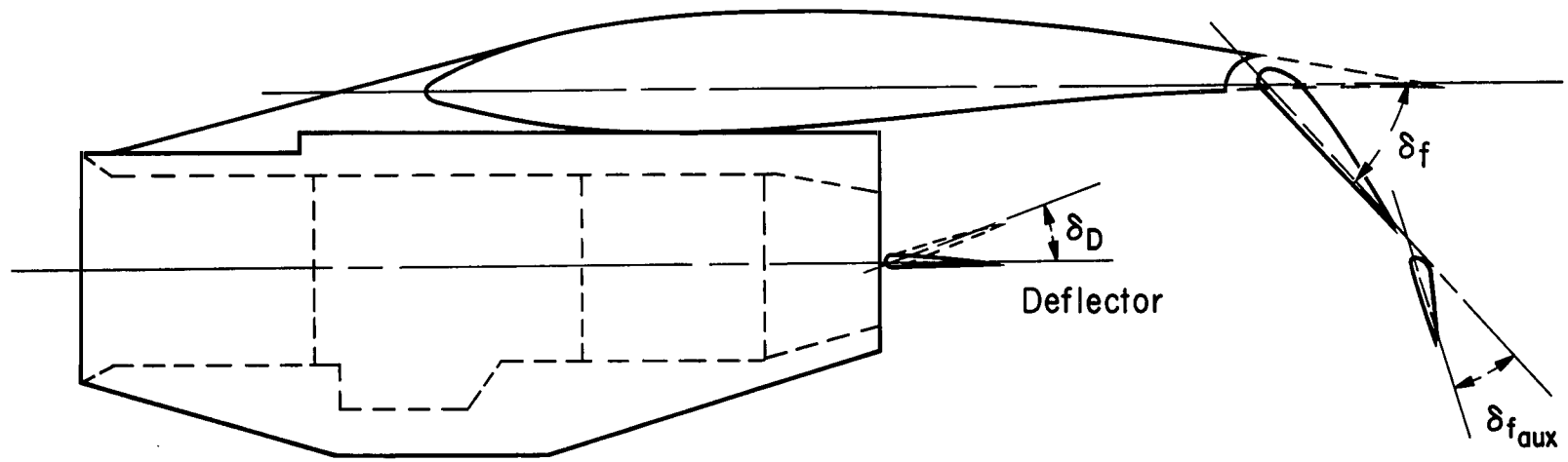
Sec B-B

Wing section		
x, in.	r, in.	s, in.
0	6.35	-2.65
5.88	5.62	-2.05
11.88	4.80	-1.45
17.88	3.75	-.92
19.50	3.50	-.20
21.50	3.15	1.95
22.50	2.99	2.51
24.38	2.70	2.63

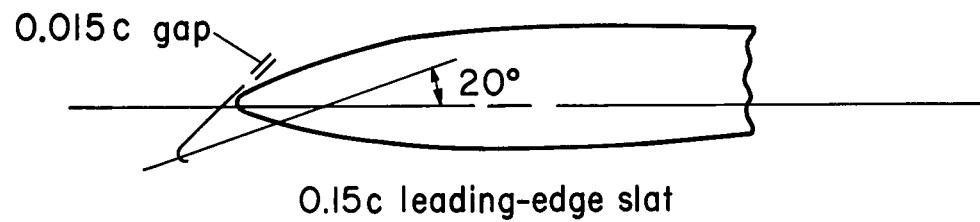
Flap		
x, in.	r, in.	s, in.
19.88	-.32	-.32
20.50	.98	-.75
21.50	1.82	-.61
22.50	2.40	—
23.50	2.63	—
24.50	2.60	-.30
29.00	1.70	.10
32.75	.89	.20
36.86	0	0

(b) Wing trailing-edge extension.

Figure 2.- Continued.



Engine nacelle and flap geometry



(c) Details of the high-lift devices.

Figure 2.- Concluded.

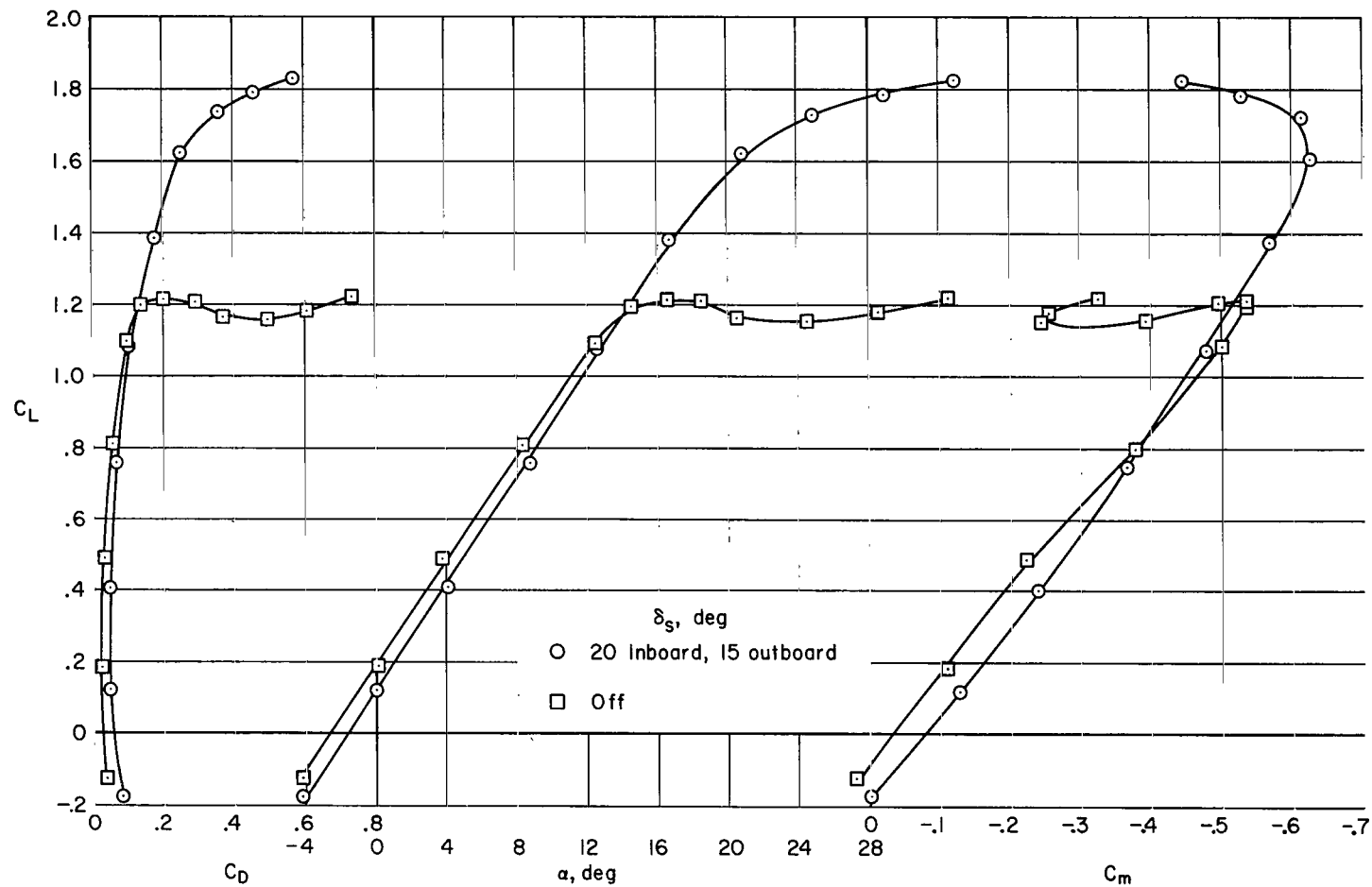


Figure 3.- The variation in longitudinal characteristics with power off; $\delta_f = 0^\circ$, $\delta_{f_{aux}} = \text{off}$, $\delta_D = 20^\circ$.

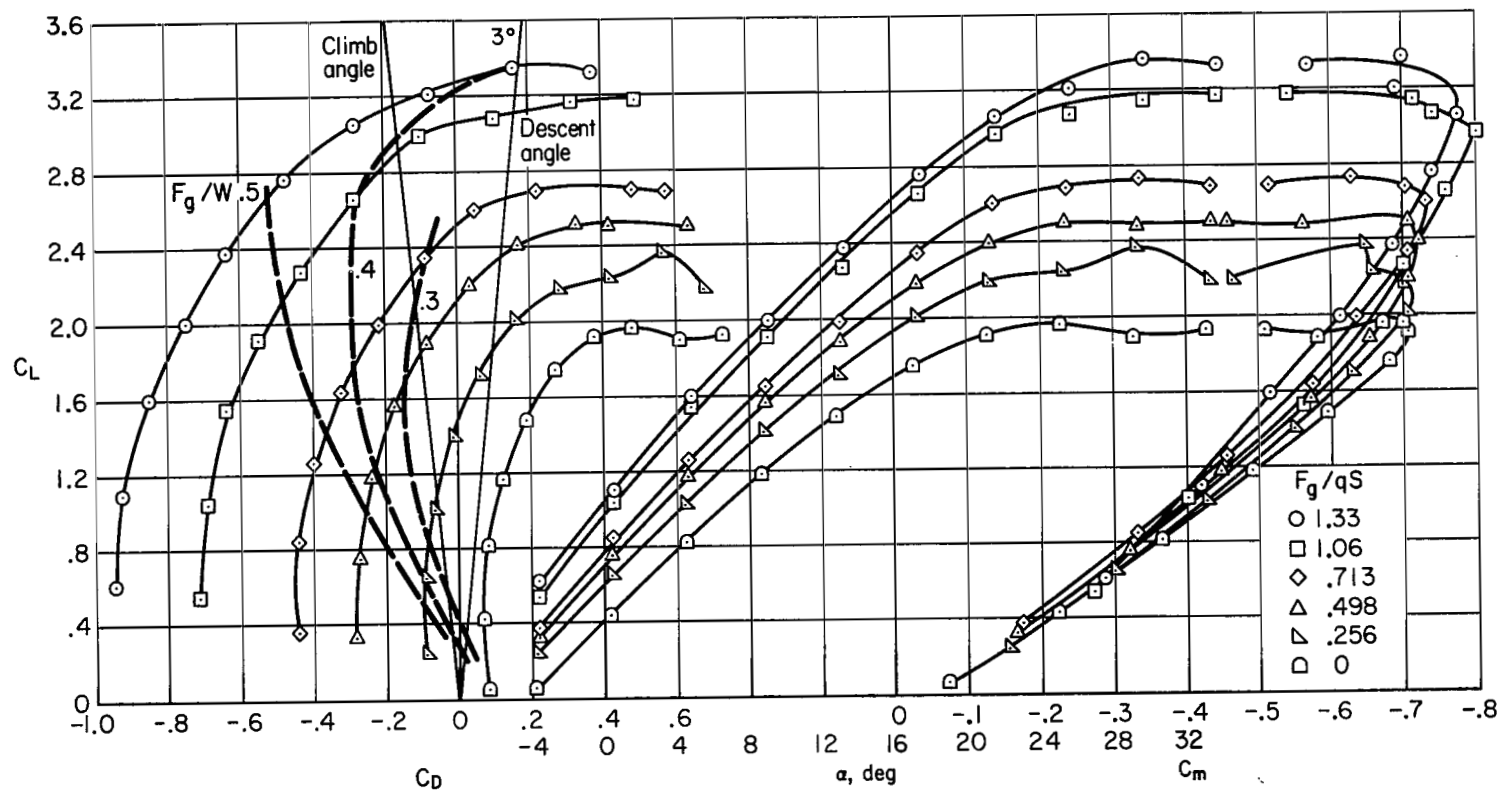


Figure 4.- The variation in longitudinal characteristics with thrust coefficient; $\delta_F = 10^\circ$, $\delta_{F_{aux}} = 20^\circ$, $\delta_D = 20^\circ$, $\delta_S = 20^\circ$.

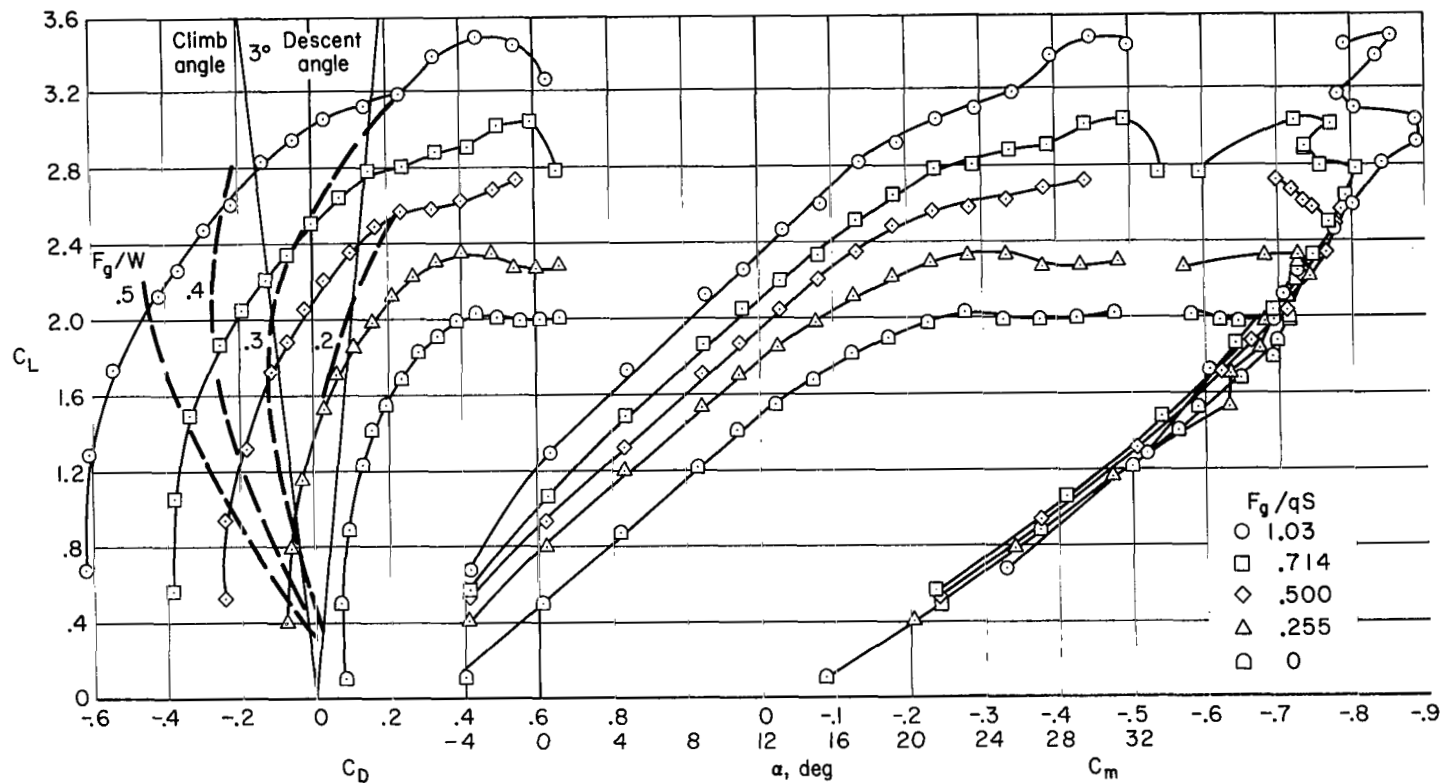


Figure 5.- The variation in longitudinal characteristics with thrust coefficient; $\delta_F = 10^\circ$, $\delta_{F_{aux}} = 30^\circ$, $\delta_D = 20^\circ$, $\delta_S = 20^\circ$.

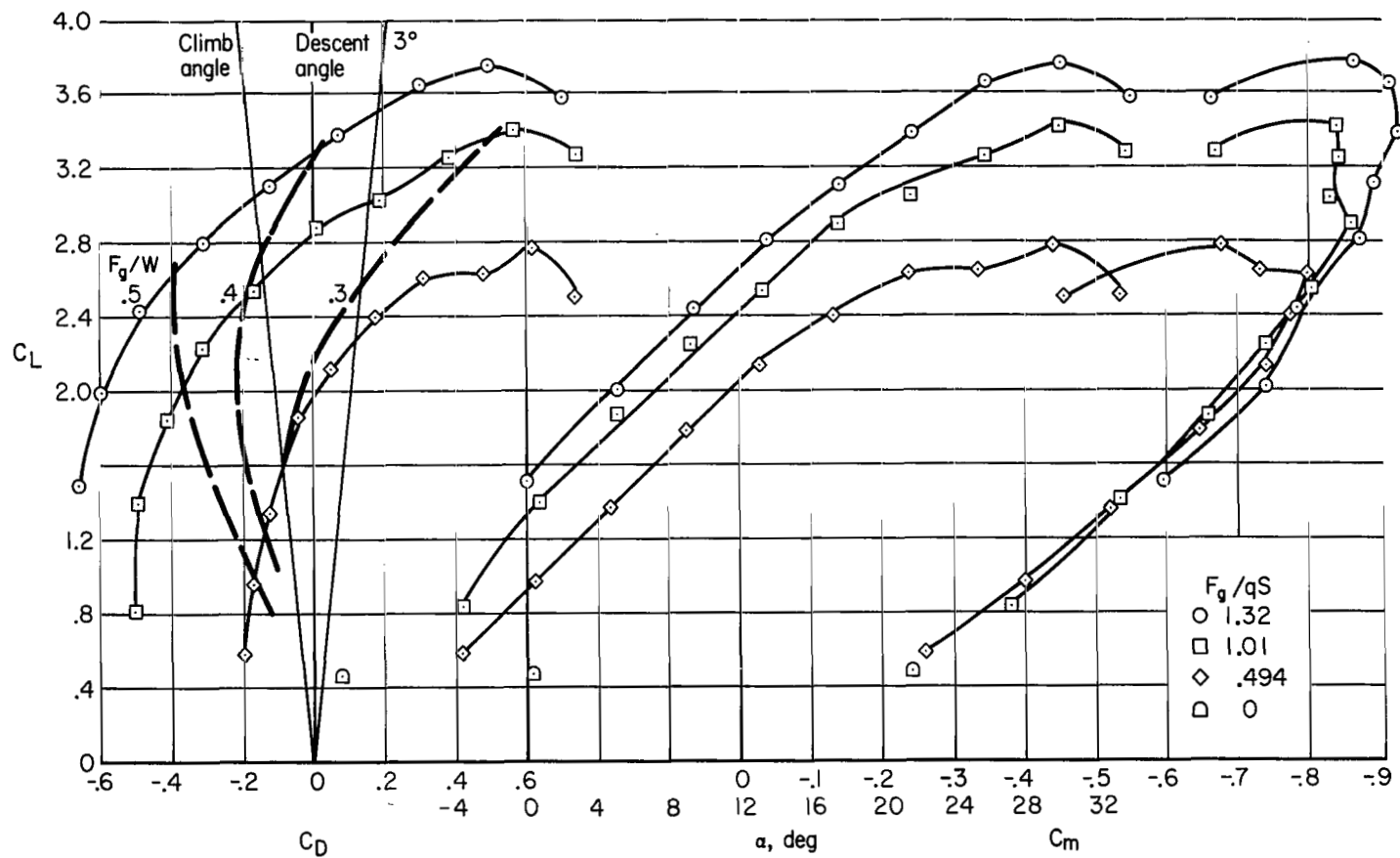


Figure 6.- The variation in longitudinal characteristics with thrust coefficient; $\delta_f = 10^\circ$, $\delta_{f_{aux}} = 40^\circ$, $\delta_D = 20^\circ$, $\delta_S = 20^\circ$.

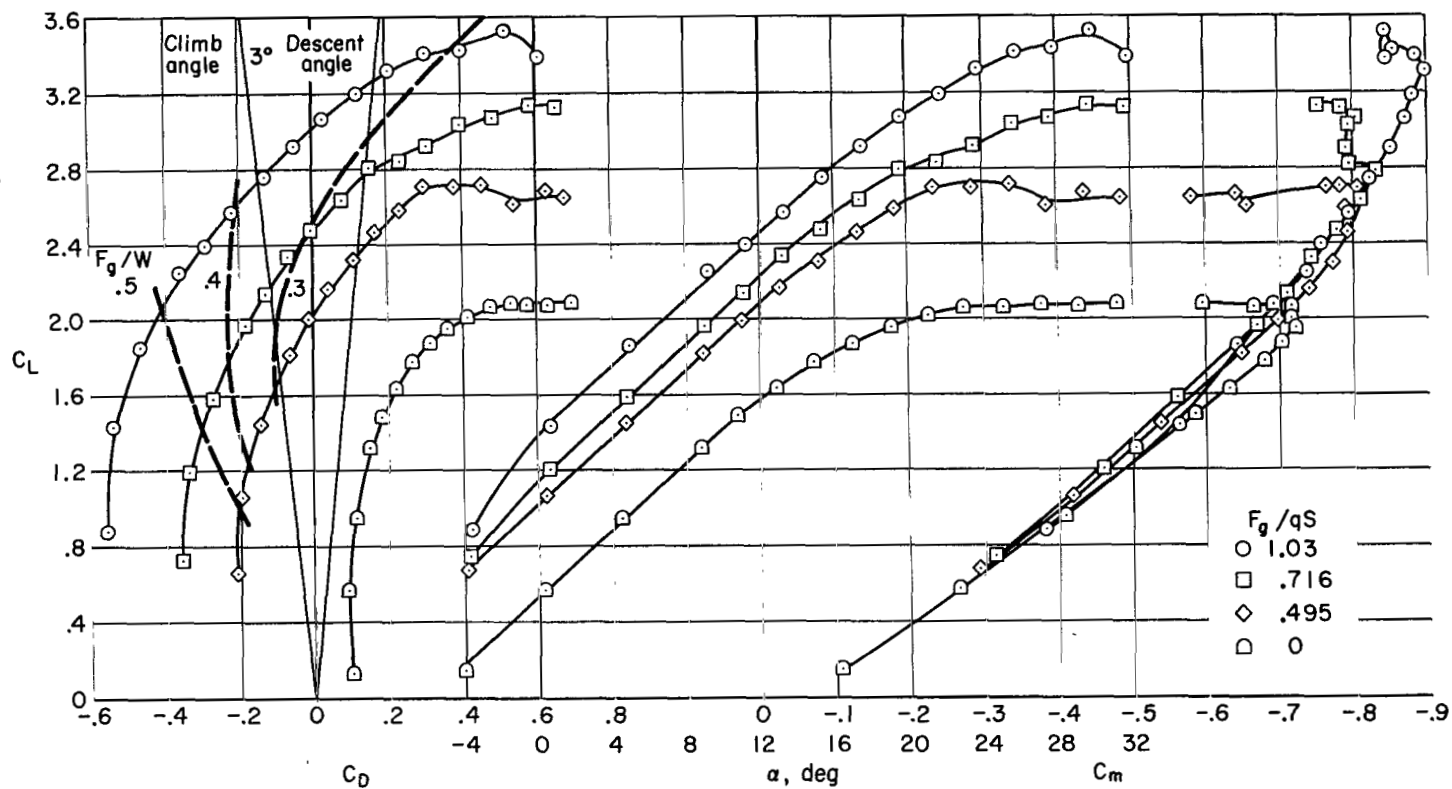


Figure 7.- The variation in longitudinal characteristics with thrust coefficient; $\delta_f = 20^\circ$, $\delta_{f_{aux}} = 20^\circ$, $\delta_D = 20^\circ$, $\delta_S = 20^\circ$.

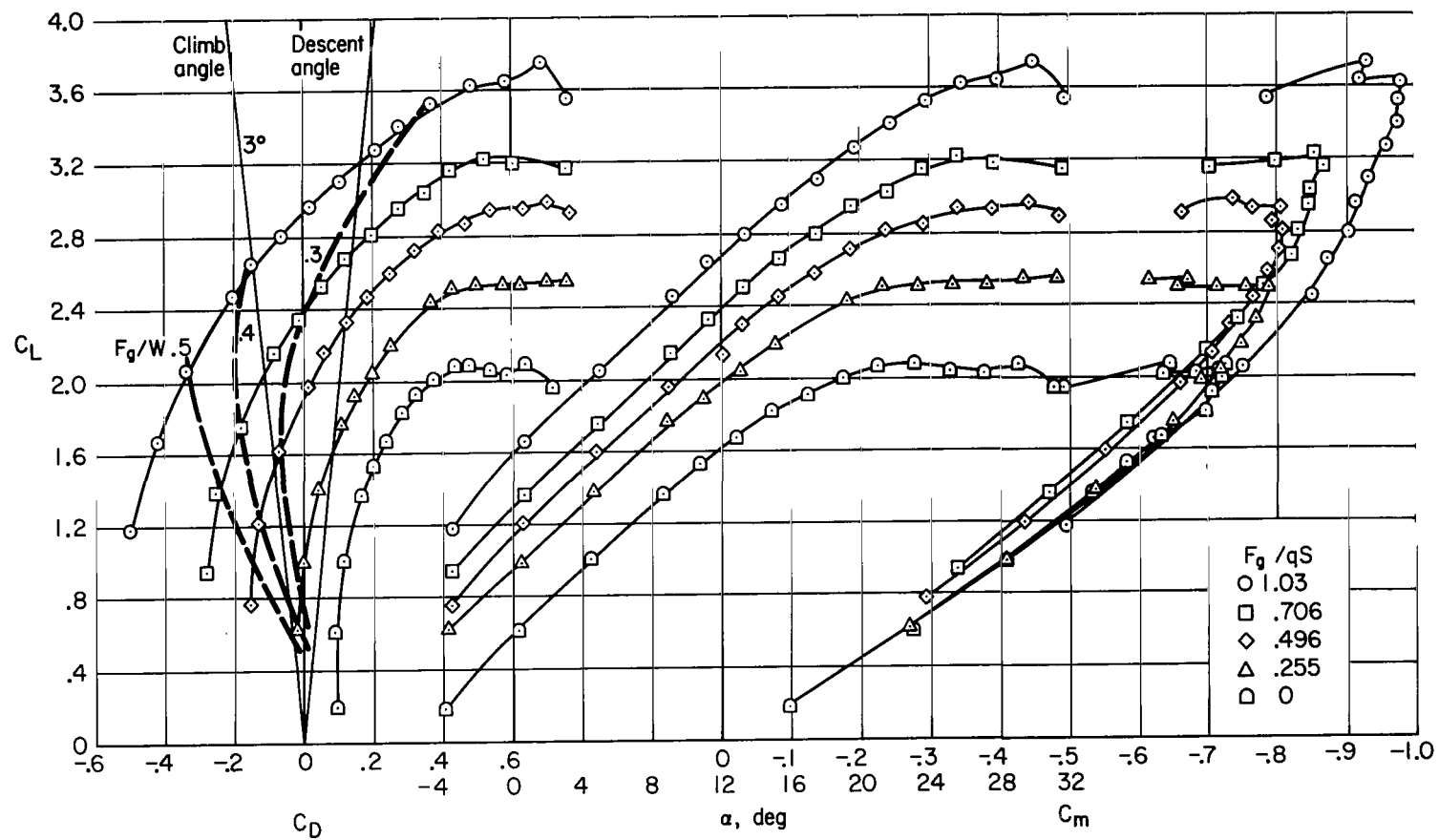


Figure 8.- The variation in longitudinal characteristics with thrust coefficient; $\delta_F = 20^\circ$, $\delta_{F_{aux}} = 30^\circ$, $\delta_D = 20^\circ$, $\delta_S = 20^\circ$.

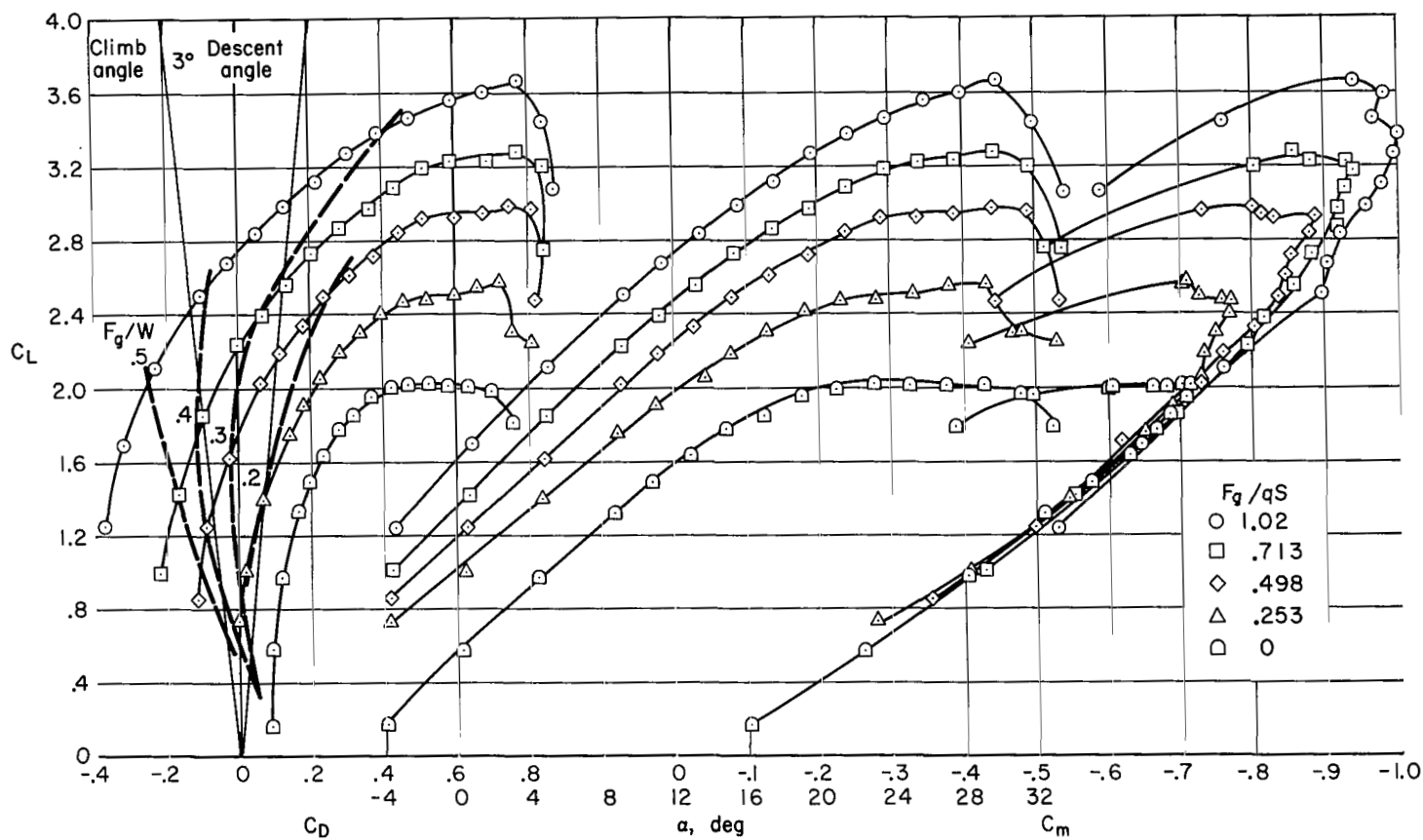


Figure 9.- The variation in longitudinal characteristics with thrust coefficient; $\delta_F = 20^\circ$,
 $\delta_{F_{aux}} = 40^\circ$, $\delta_D = 20^\circ$, $\delta_S = 20^\circ$.

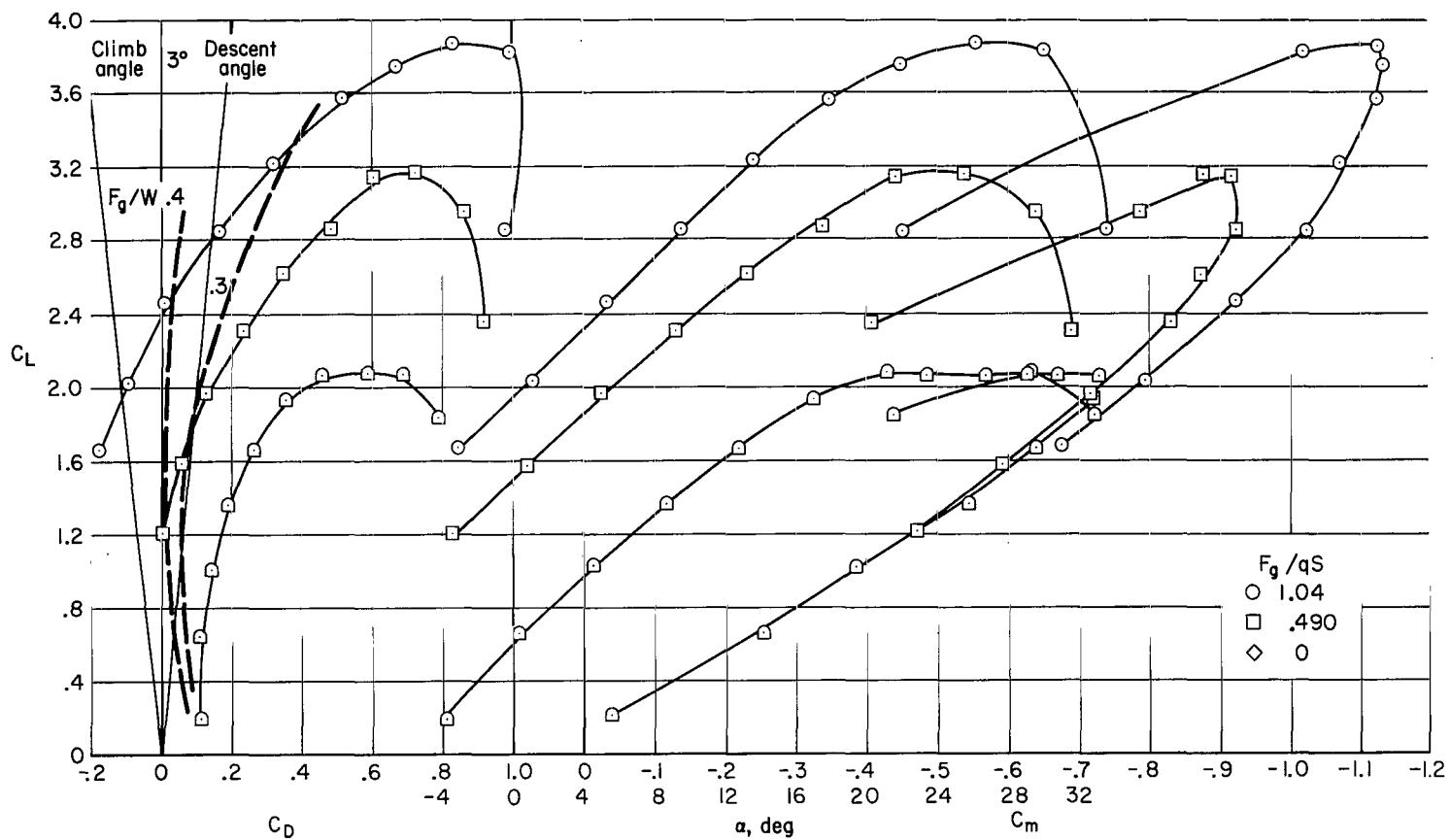


Figure 10.- The variation in longitudinal characteristics with thrust coefficient; $\delta_F = 40^\circ$, $\delta_{F_{aux}} = 20^\circ$, $\delta_D = 20^\circ$, $\delta_S = 20^\circ$.

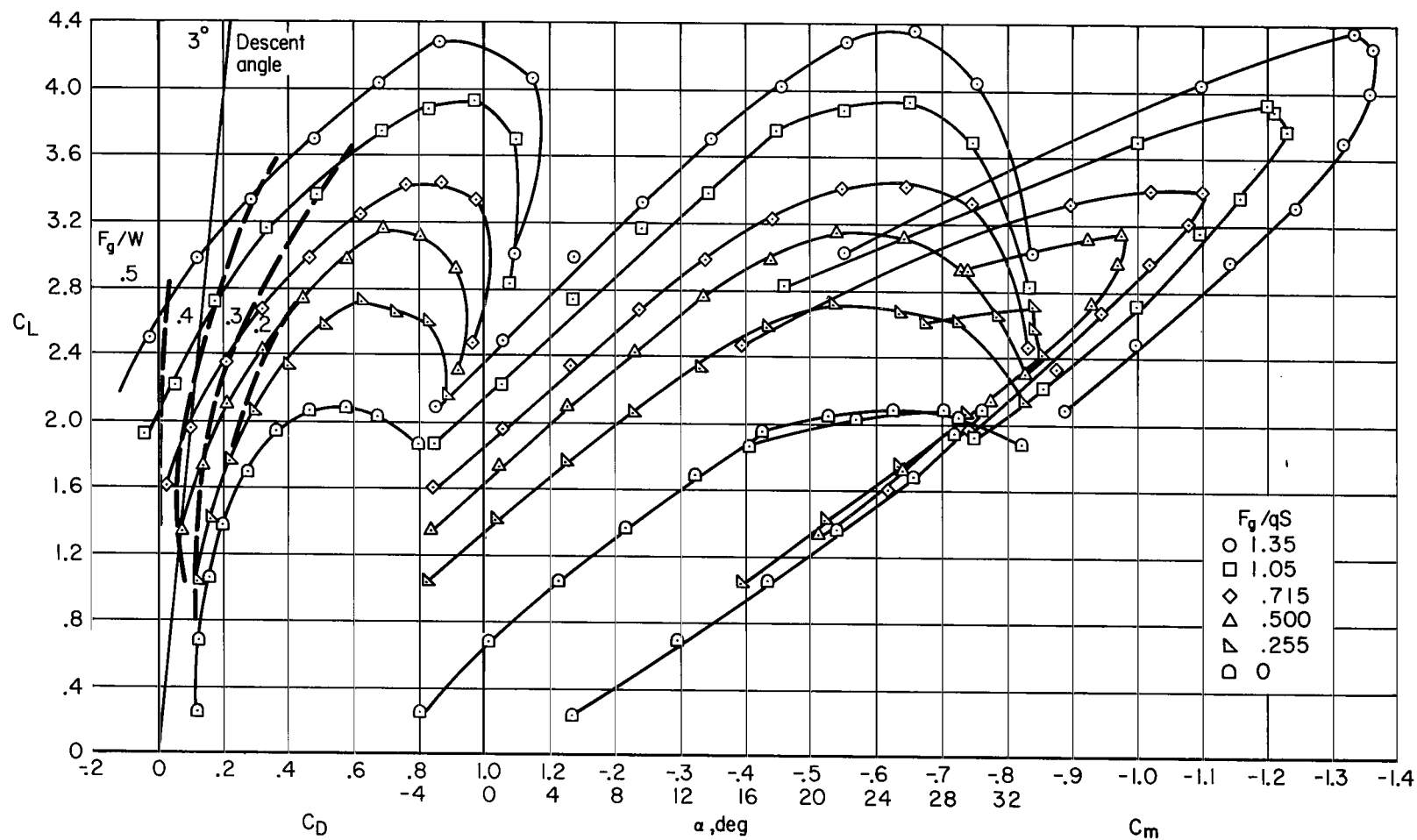


Figure 11.- The variation in longitudinal characteristics with thrust coefficient; $\delta_F = 40^\circ$, $\delta_{F_{aux}} = 30^\circ$, $\delta_D = 20^\circ$, $\delta_S = 20^\circ$.

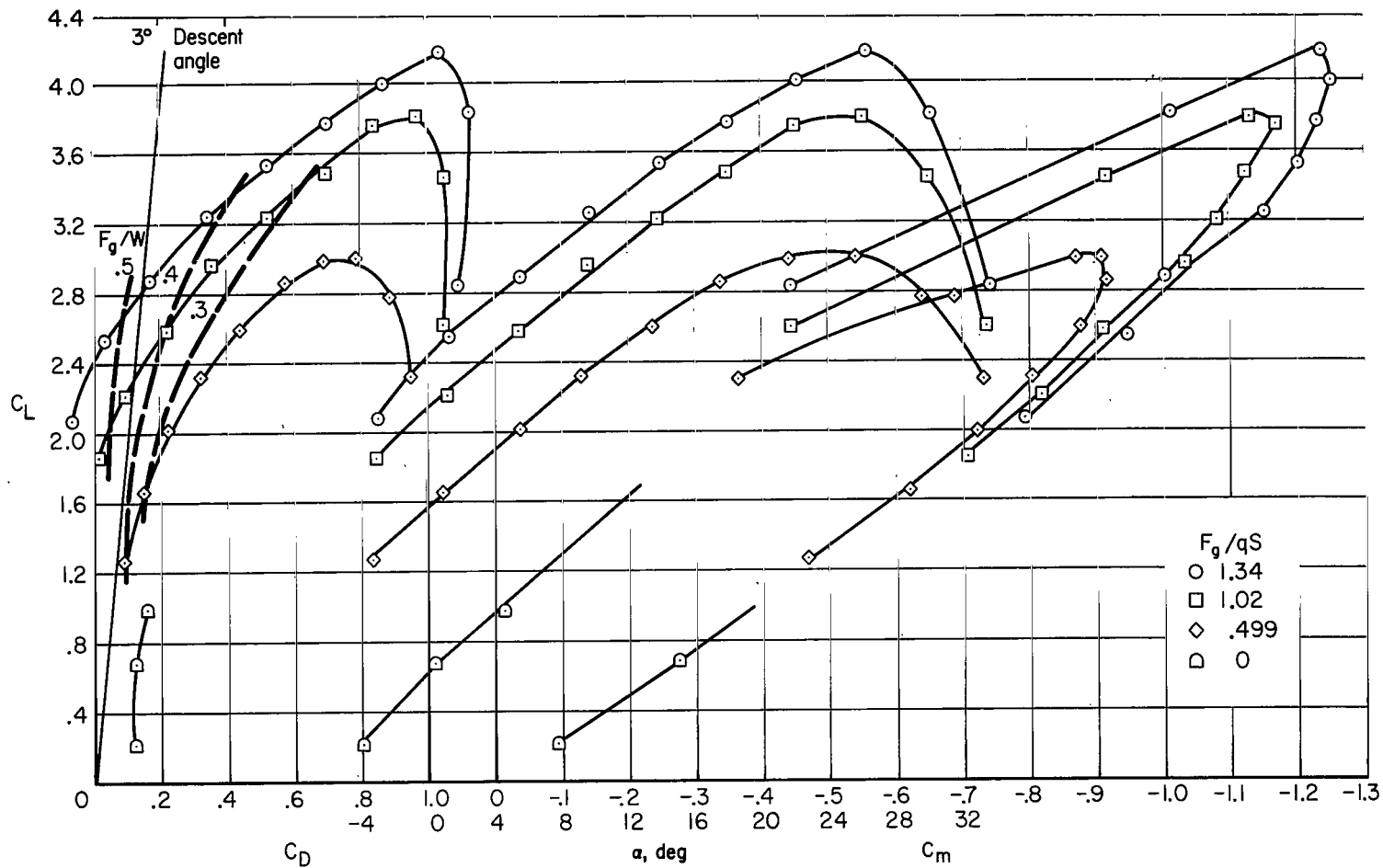


Figure 12.- The variation in longitudinal characteristics with thrust coefficient; $\delta_f = 40^\circ$, $\delta_{f_{aux}} = 40^\circ$, $\delta_D = 20^\circ$, $\delta_S = 20^\circ$.

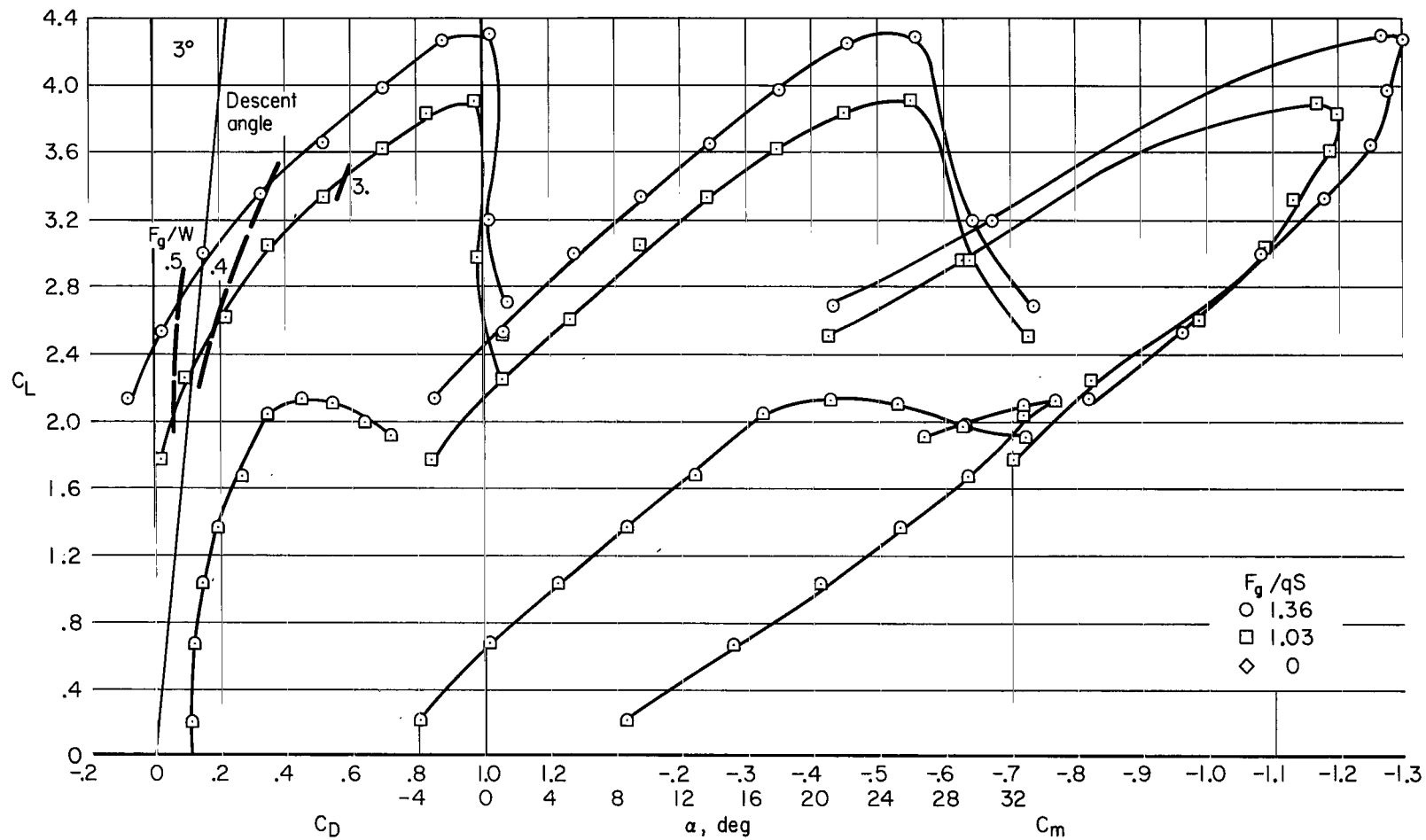


Figure 13.- The variation in longitudinal characteristics with thrust coefficient; $\delta_F = 40^\circ$, $\delta_{F_{aux}} = 40^\circ$, $\delta_D = 20^\circ$, $\delta_S = 20^\circ$ inboard/15° outboard.

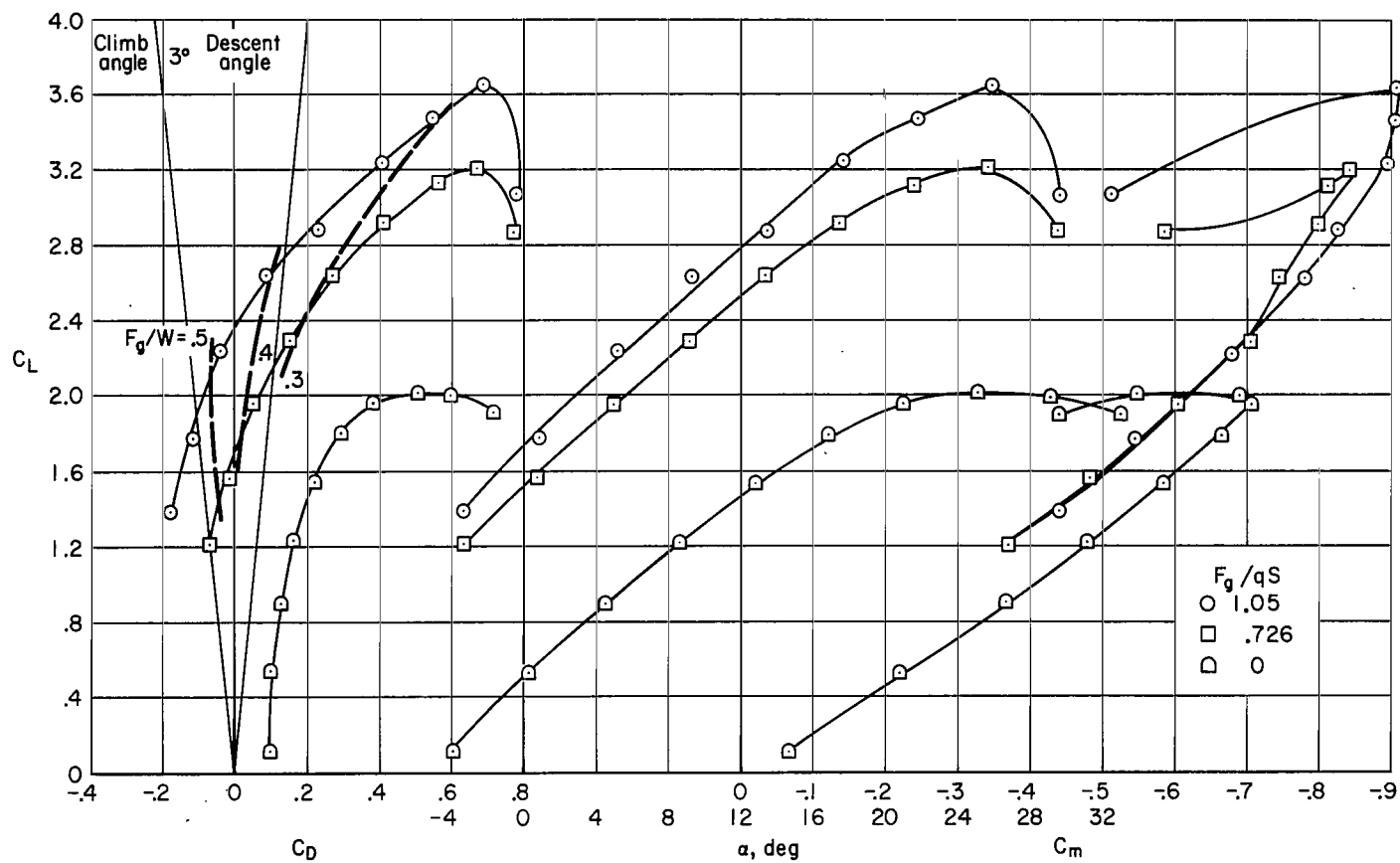
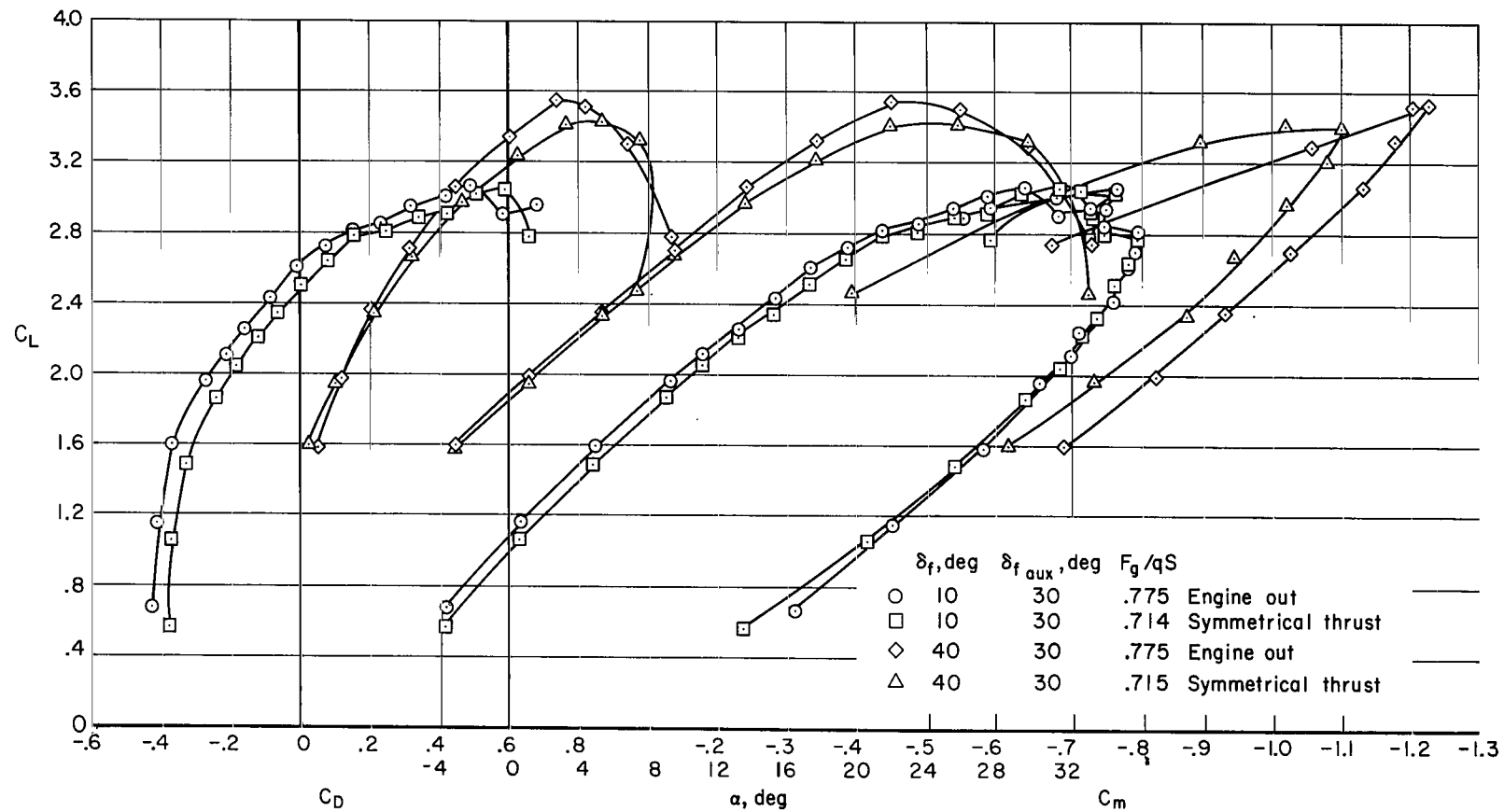
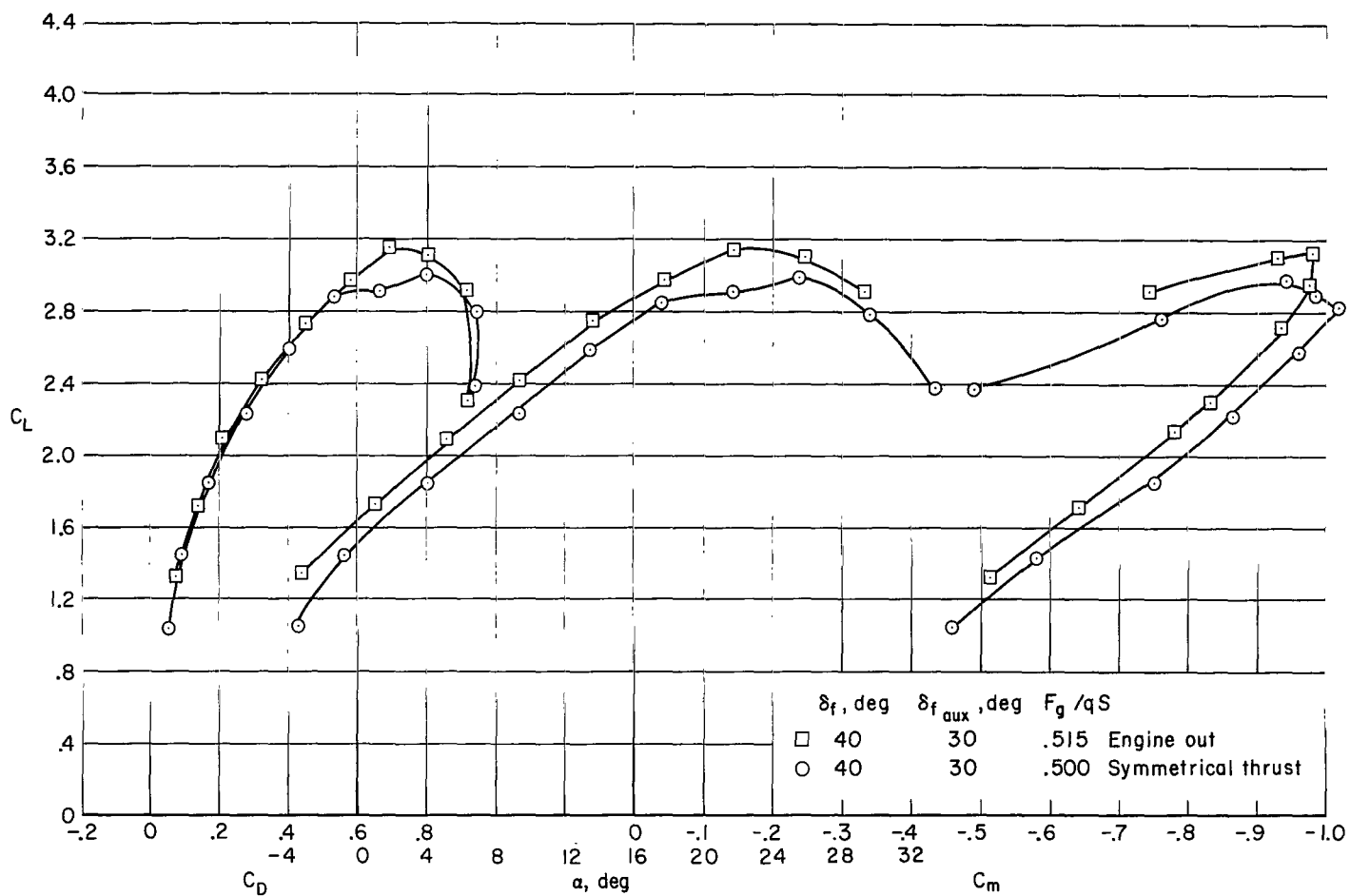


Figure 14.- The variation in longitudinal characteristics with thrust coefficient; $\delta_f = 60^\circ$, $\delta_{f_{aux}} = \text{off}$, $\delta_D = 20^\circ$, $\delta_S = 20^\circ$ inboard/ 15° outboard.



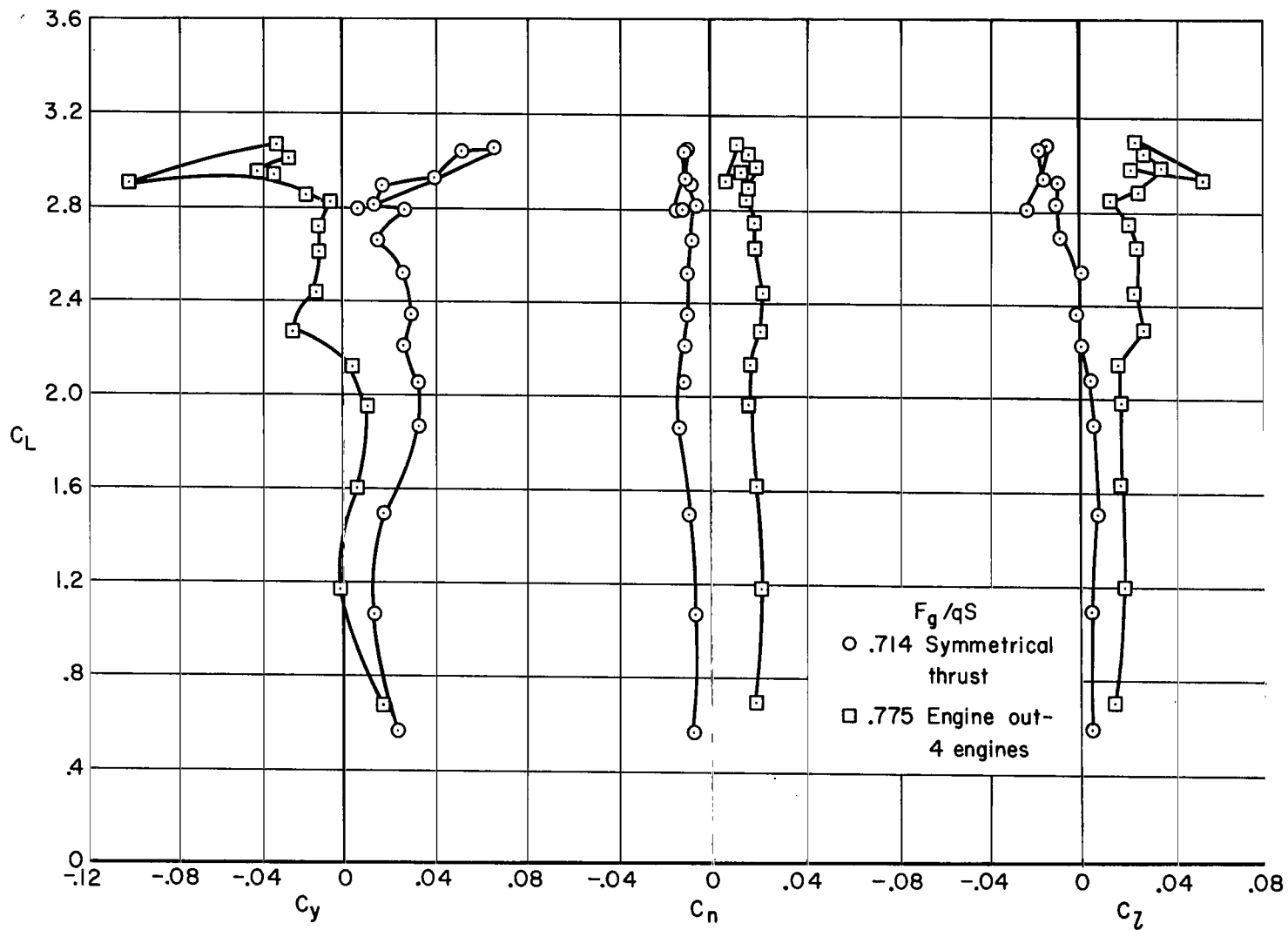
(a) Four engine simulation.

Figure 15.- The variation in longitudinal characteristics during engine out simulation; $\delta_D = 20^\circ$, $\delta_S = 20^\circ$.



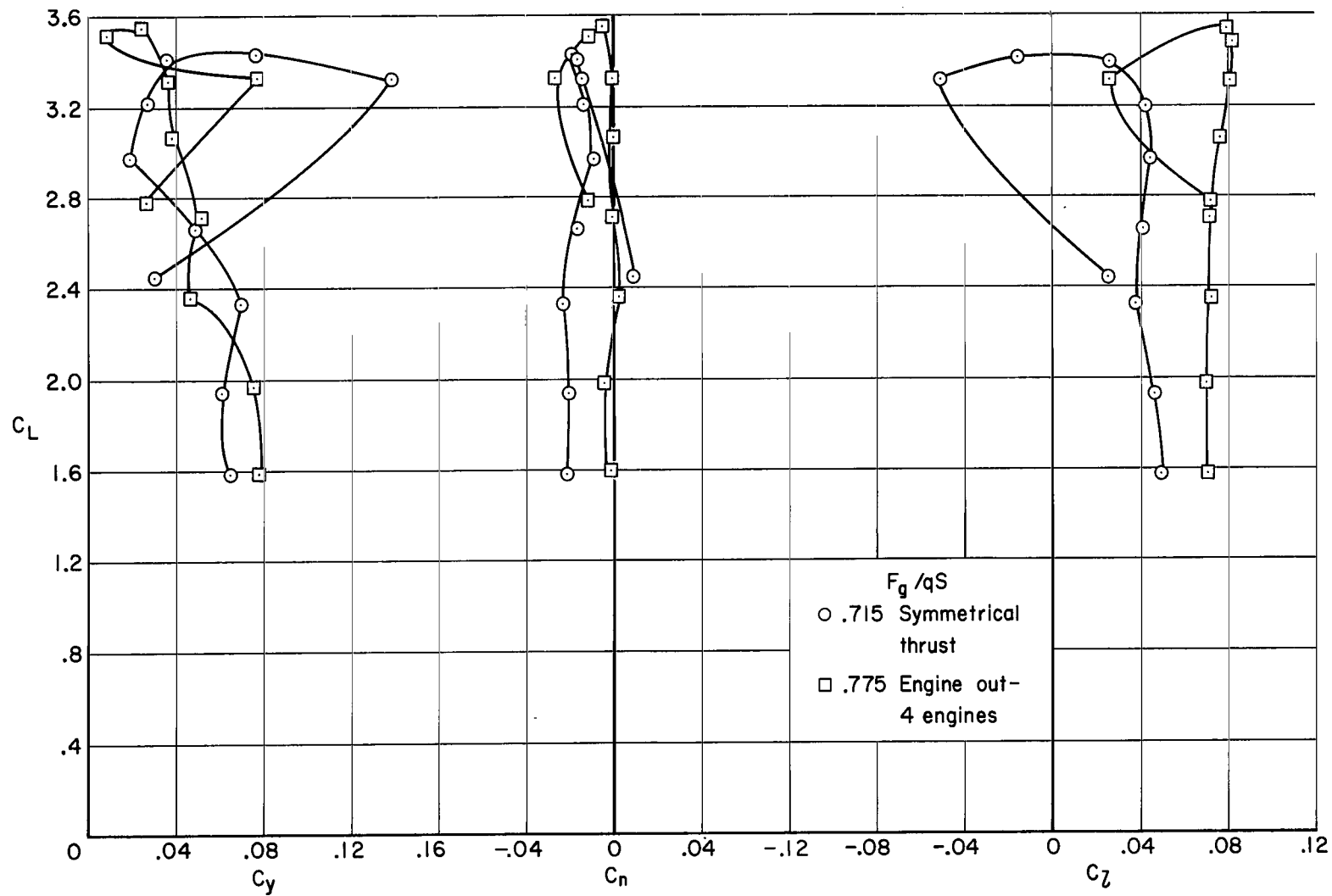
(b) Two engine simulation.

Figure 15.- Concluded.



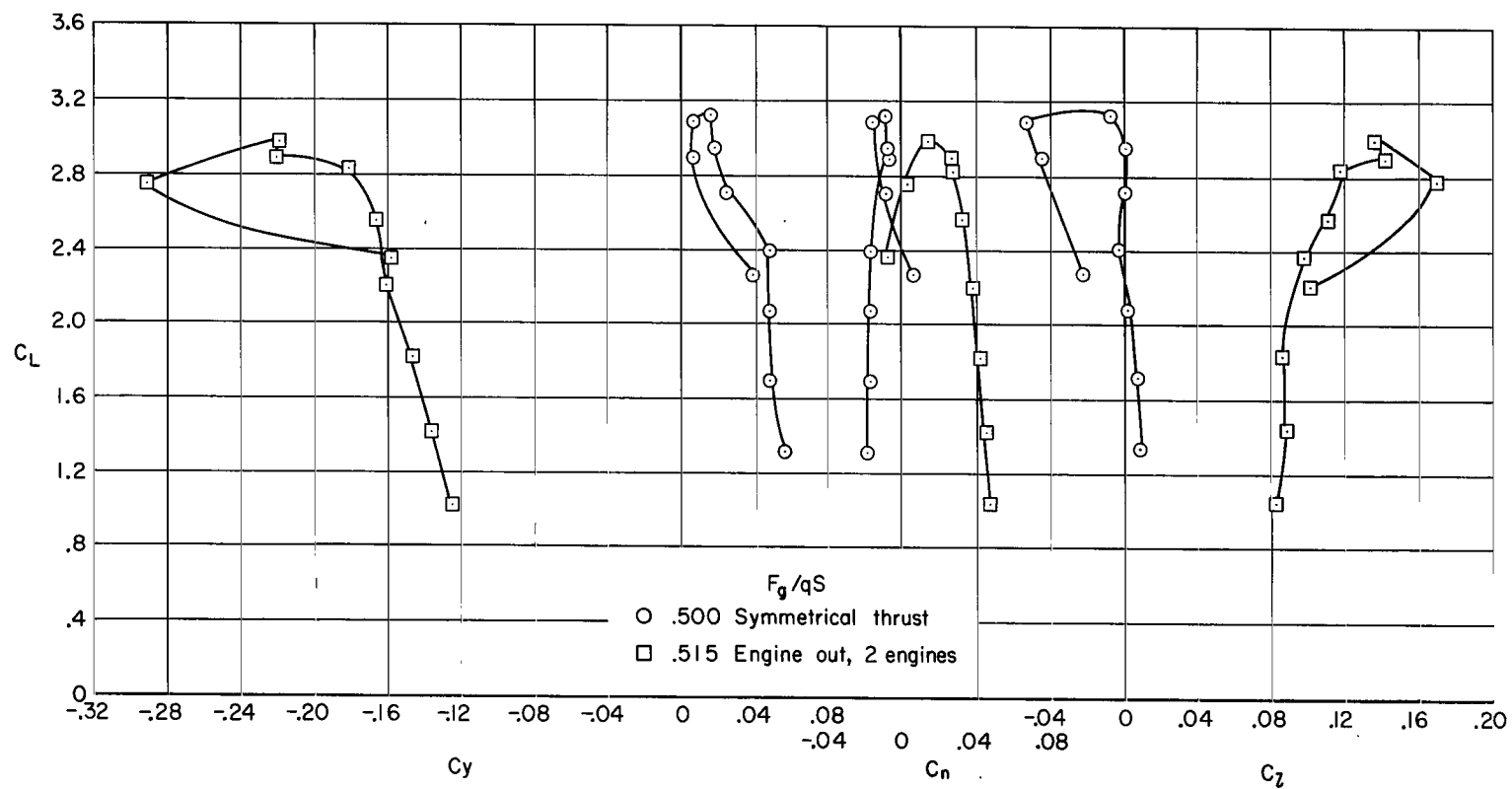
(a) $\delta_F = 10^\circ$, $\delta_{F_{aux}} = 30^\circ$

Figure 16.- The variation in lateral-directional characteristics during engine out simulation;
 $\delta_D = 20^\circ$, $\delta_S = 20^\circ$.



(b) $\delta_f = 40^\circ$, $\delta_{f_{aux}} = 30^\circ$

Figure 16.- Continued.



(c) $\delta_F = 40^\circ$, $\delta_{F_{aux}} = 30^\circ$

Figure 16.- Concluded.

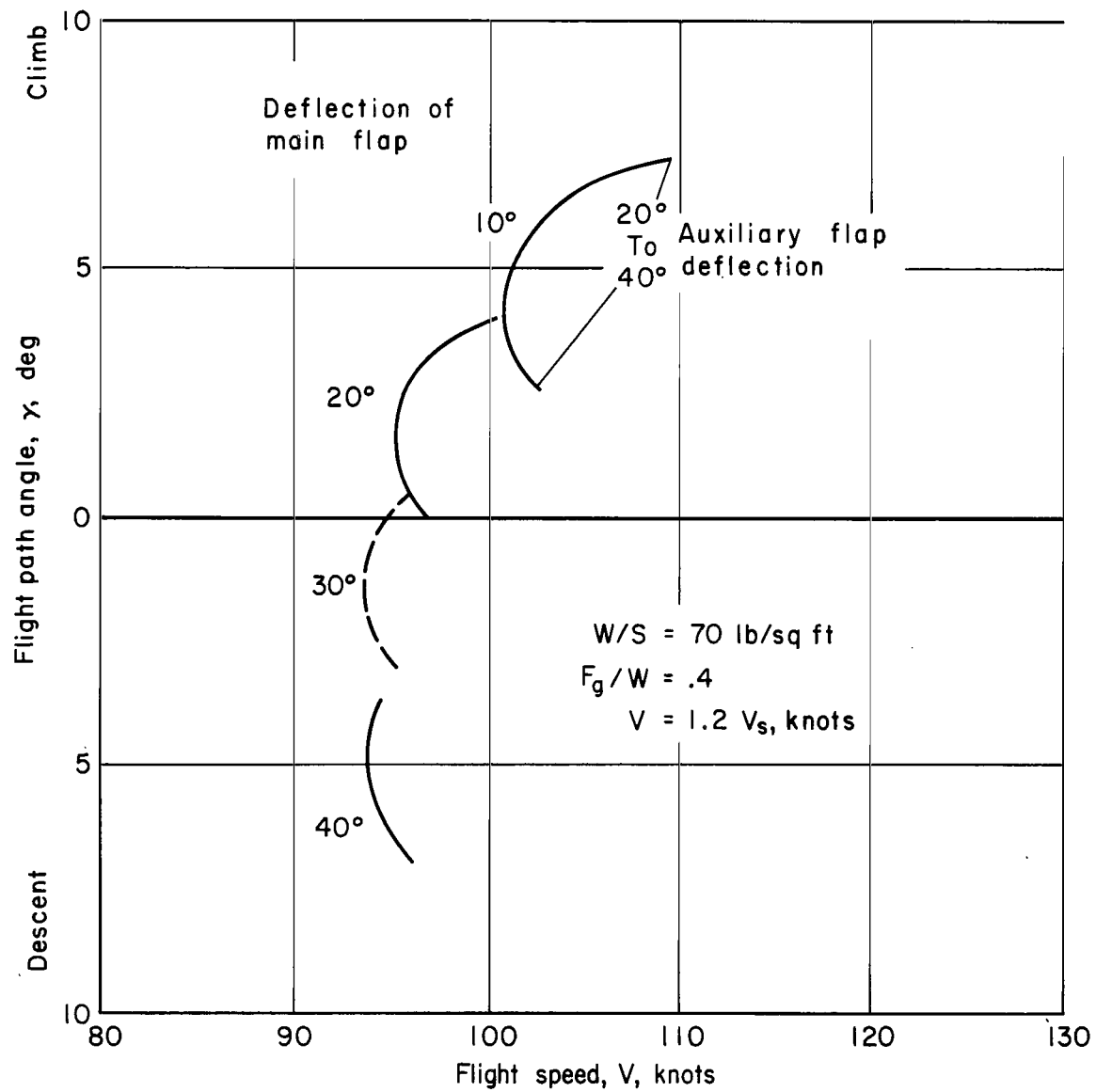


Figure 17.- Flight path control with auxiliary flap deflection.

"The aeronautical and space activities of the United States shall be conducted so as to contribute . . . to the expansion of human knowledge of phenomena in the atmosphere and space. The Administration shall provide for the widest practicable and appropriate dissemination of information concerning its activities and the results thereof."

—NATIONAL AERONAUTICS AND SPACE ACT OF 1958

NASA SCIENTIFIC AND TECHNICAL PUBLICATIONS

TECHNICAL REPORTS: Scientific and technical information considered important, complete, and a lasting contribution to existing knowledge.

TECHNICAL NOTES: Information less broad in scope but nevertheless of importance as a contribution to existing knowledge.

TECHNICAL MEMORANDUMS: Information receiving limited distribution because of preliminary data, security classification, or other reasons.

CONTRACTOR REPORTS: Scientific and technical information generated under a NASA contract or grant and considered an important contribution to existing knowledge.

TECHNICAL TRANSLATIONS: Information published in a foreign language considered to merit NASA distribution in English.

SPECIAL PUBLICATIONS: Information derived from or of value to NASA activities. Publications include conference proceedings, monographs, data compilations, handbooks, sourcebooks, and special bibliographies.

TECHNOLOGY UTILIZATION PUBLICATIONS: Information on technology used by NASA that may be of particular interest in commercial and other non-aerospace applications. Publications include Tech Briefs, Technology Utilization Reports and Notes, and Technology Surveys.

Details on the availability of these publications may be obtained from:

SCIENTIFIC AND TECHNICAL INFORMATION DIVISION
NATIONAL AERONAUTICS AND SPACE ADMINISTRATION
Washington, D.C. 20546